



LAWRENCE  
LIVERMORE  
NATIONAL  
LABORATORY

# Detecting Objects With Partial Obstruction at the ARC Split Beam Injector Images at the National Ignition Facility

A. Awwal, R. Leach, R. Roberts, K. Wilhelmsen,  
D. McGuigan, J. Jarboe

August 28, 2014

SPIE Optics and Photonics  
San Diego, CA, United States  
August 17, 2014 through August 21, 2014

## **Disclaimer**

---

This document was prepared as an account of work sponsored by an agency of the United States government. Neither the United States government nor Lawrence Livermore National Security, LLC, nor any of their employees makes any warranty, expressed or implied, or assumes any legal liability or responsibility for the accuracy, completeness, or usefulness of any information, apparatus, product, or process disclosed, or represents that its use would not infringe privately owned rights. Reference herein to any specific commercial product, process, or service by trade name, trademark, manufacturer, or otherwise does not necessarily constitute or imply its endorsement, recommendation, or favoring by the United States government or Lawrence Livermore National Security, LLC. The views and opinions of authors expressed herein do not necessarily state or reflect those of the United States government or Lawrence Livermore National Security, LLC, and shall not be used for advertising or product endorsement purposes.

# Detecting objects with partial obstruction at the ARC split beam injector images at the National Ignition Facility

Abdul A. S. Awwal, Richard R. Leach Jr., Randy S. Roberts, Karl Wilhelmsen, David McGuigan,  
and Jeff Jarboe

Integrated Computer Control System, National Ignition Facility  
Computational Engineering Division  
Lawrence Livermore National Laboratory, Livermore, CA. 94551  
*E-mail:* [awwal1@llnl.gov](mailto:awwal1@llnl.gov)

## ABSTRACT

The National Ignition Facility (NIF) utilizes 192 beams, four of which are diverted to create the Advanced Radiographic Capability (ARC) by generating a sequence of *short laser pulses*. This ARC beam after being converted to X-rays will act as a back lighter to create a radiographic movie and provide an unprecedented insight into the imploding dynamics and serve as a diagnostic for tuning the experimental parameters to achieve fusion. One such beam is the centering beam of the pre-amplifier module which due to a split path obstructs the central square alignment fiducials. This fiducial is used for alignment and also as reference for the programmable spatial shaper (PSS) system. Image processing algorithms are used to process the images and calculate the position of various fiducials in the beam path. We discuss the algorithm to process ARC split beam injector (SBI) centering images with partial fiducial information.

Key words: Optical alignment, pattern recognition, Laser alignment, image processing, correlation, matched filtering, programmable spatial shaper, spatial light modulator

## 1. INTRODUCTION

The Advanced Radiographic Capability (ARC) at National Ignition Facility (NIF) was developed to produce a sequence of *short laser pulses* in order to backlight an imploding target at the target chamber center [1,2]. The back lighter beam, after being converted to X-rays, will provide an unprecedented understanding of the target implosion and the parameters affecting the quality of the implosion. The back lighter beam will create a radiographic movie of the imploding target and serve as a diagnostic for tuning the experimental parameters to achieve fusion.

For proper operation of the ARC, the beams must be aligned properly. One such beam is the centering beam of the pre-amplifier module (PAM) which, due to a split path obstructs the central square alignment fiducials as shown in Figure 1. This fiducial is used for alignment and also as reference for the programmable spatial shaper (PSS) system. The integrated automated control system aligns 192 NIF beam positions by controlling mirrors and other devices to adjust the beam positions to desired reference locations [3,4,5]. Beam and reference positions are calculated by image analysis algorithms which process the beam and reference images collected by CCD cameras. This work presents the algorithm for processing ARC split beam injector (SBI) centering images with partial fiducial information.

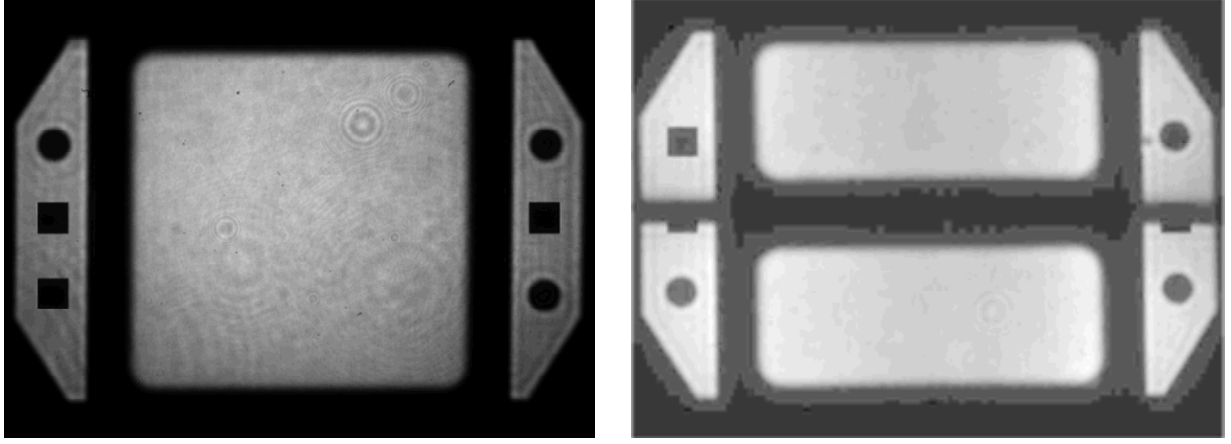


Figure 1: (a) A PAM alignment image (b) ARC SBI alignment image with enhanced low light levels

## 2. BACKGROUND

The classical or complex matched filter (CMF) is well known for its position detection capability where the position of the object is actually the position of the correlation peak as will be explained later. A CMF [6] can be defined by assuming that the Fourier transform of the object function  $f(x,y)$  is denoted by:

$$F(U_x, U_y) = |F(U_x, U_y)| \exp(j\Phi(U_x, U_y)) \quad (1)$$

The CMF for detecting the function  $f(x,y)$  and its location, is given by the complex conjugate of the Fourier spectrum  $F(U_x, U_y)$  as denoted in Eq. 2,

$$H_{CMF}(U_x, U_y) = F^*(U_x, U_y) = |F(U_x, U_y)| \exp(-j\Phi(U_x, U_y)) \quad (2)$$

The shape of correlation and the discrimination capability of CMF are usually not as good as that of a phase only filter or amplitude modulated correlation filter [6,7]. The position accuracy and detection capability of the CMF can be further enhanced by constructing the matched filter (Eq. 2) from the edges of the fiducial and operating on edge-detected preprocessed image.

The position of the object can be found from the position of the cross correlation, autocorrelation, and the position of the template using Eqs. 3(a-b).

$$X_{pos} = X_{cross} - X_{auto} + X_c \quad (3a)$$

$$Y_{pos} = Y_{cross} - Y_{auto} + Y_c \quad (3b)$$

where  $(x_{pos}, y_{pos})$  is the to-be-determined position of the pattern in the image plane,  $(x_{auto}, y_{auto})$  is the position of the template autocorrelation peaks and  $(x_{cross}, y_{cross})$  is the position of the cross correlation peak. The position of the cross-correlation peak is estimated using a polynomial fit of second order to the correlation peak. The center of the template,  $(x_c, y_c)$ , and  $(x_{auto}, y_{auto})$  are calculated off-line. An illustration of the equation 3a-b is depicted in Fig. 2. A pulse shown

on the top left of Fig. 2, is assumed to be the template, centered on  $x_c = 15$ . By default the origin is assumed to be at 0. When an autocorrelation is performed, the resulting correlation function will be a triangular pulse centered on 0. In an optical or 2-D digital processing, the origin of the output plane is usually centered on the middle of the plane. Shifting the origin to a hypothetical point 300, we get  $x_{\text{auto}} = 300$ . Now imagine we want to detect a pulse located at 605. The cross-correlation of the input with the to-be-detected pulse will be centered on 890 at the shifted origin of 300. It is a simple exercise to verify that the pulse position (605) can be obtained easily from the values of the cross, auto and template position. This same technique is applied in detecting a 2-D object except the same calculation is extended to a 2-D image plane.

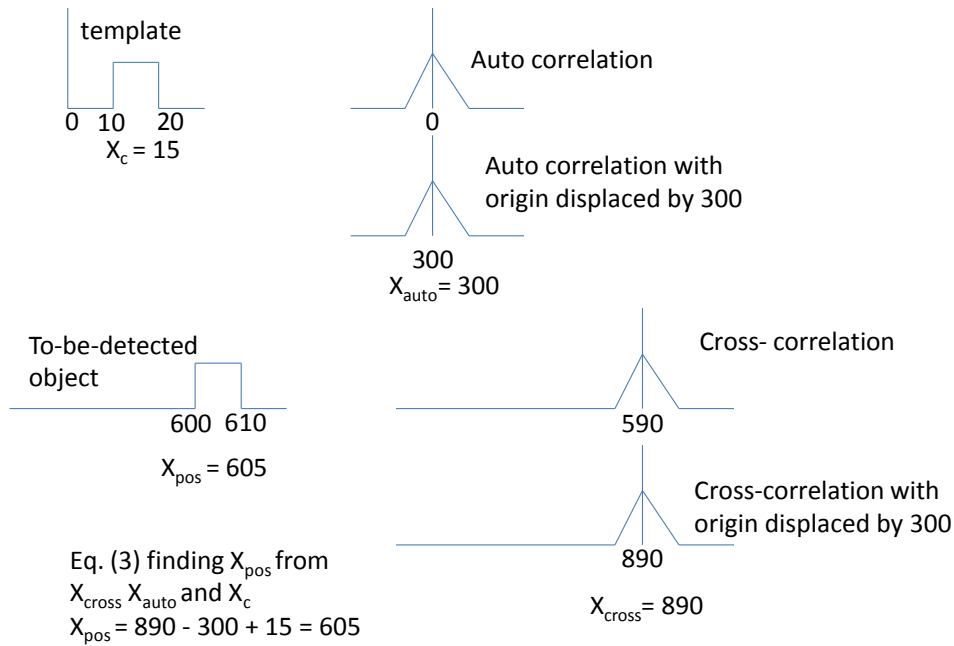


Figure 2: Relationship of positions of correlation peak with those of the template and the assumed origin location in 1-D.

### 3. ALGORITHMS

A NIF preamplifier module (PAM) alignment image is depicted in Fig. 1a. The beam is straddled by two alignment wings consisting of three fixed-position square fiducials representing a reference position and three circles that move with beam position. A NIF preamplifier is aligned by moving the beam such that the square and circular fiducials are aligned as shown in Fig. 1a. The ARC produces two beams that are combined into a single NIF beam by a Split Beam Injector (SBI). As shown in Fig 1b., the ARC beams are positioned one over the other in the same space as a NIF beam. This optical arrangement allows ARC to use the same PAM as NIF. However, the gap between the upper and lower ARC beams obscures the square fiducials that are normally used to align a NIF beam in the PAM. Thus, the normal image processing used in the PAM alignment will no longer work and new algorithms are required for aligning ARC into the PAM.

The beam portion is represented by the inner illuminated square. The three alignment fiducial circles are designed to move with the beam. The reference square fiducials remains static. When the midpoint of the two diagonal circles coincides with the center of the two square fiducials at the middle, the beam is aligned. When an offset is requested, the difference between the two is equal to the offset. The difference between these two positions and any desired offset serves as the error signal used to drive the control system to perform auto-alignment.

All NIF algorithms must perform a preprocessing in order to eliminate any false, black, white or truncated images. This is done in the off-normal detection stage [8]. When an image is found to be normal, it is passed to the matched-filter algorithm [9], which processes the image and finds the location of the fiducials. If the position of each type of fiducial is accepted after the error checking and correction step, the algorithm outputs the positions of all the fiducials with their corresponding uncertainty [10].

The off-normal processor uses statistical methods to classify and detect simple black, white or dim images. In addition, the off-normal processor checks for the size of the beam using average intensity profiles along the x- and y-direction. Historic image sets are analyzed to determine the nominal values of all the beam parameters such as mean and max of intensity levels, min and max of sizes, etc. [8]. For example, the length ( $l$ ) of the ARC SBI beam is measured to make sure there is a valid beam between 320 and 450 pixels wide.

$$l_{\text{lower}} < l_{\text{FWHM}} < l_{\text{upper}} \quad (4)$$

where,  $l_{\text{lower}} = 320$  and  $l_{\text{upper}} = 450$ . To keep the operation of off-normal processor up-to-date, off-normal images of various kinds are periodically added to a database. These images are used as test images for the algorithm before it is released to the NIF facility.

The algorithm is designed to determine the position of the two different fiducials for alignment. Due to varying imaging conditions and optical distortions, the circles and squares could vary in size. Thus the template for the matched filtering algorithm is determined adaptively for every beam line.

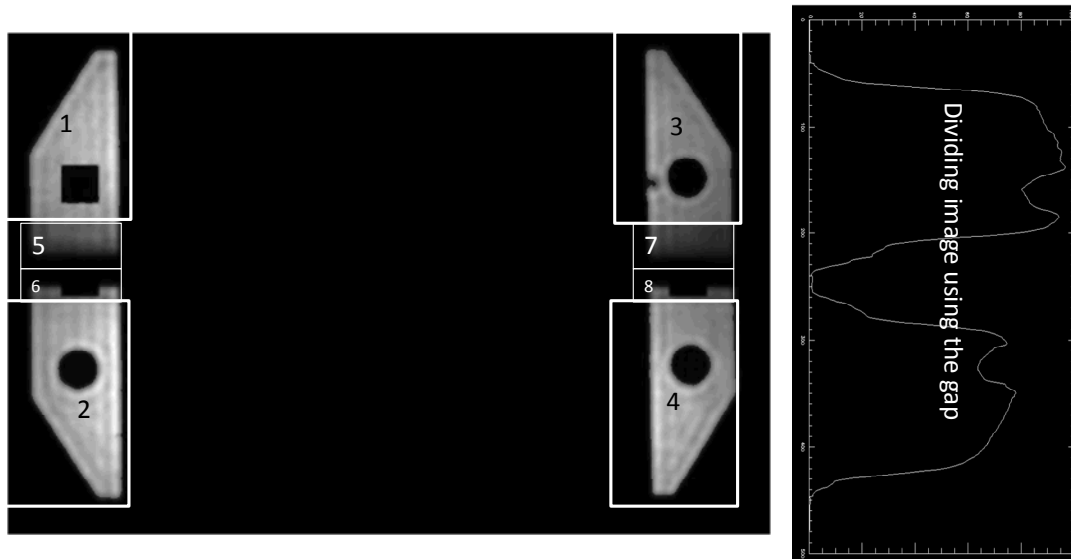


Figure 3: 8 segments of the ARC SBI image

The first step in processing the ARC SBI image is to remove the center of the image. Thereafter it is divided into 8 subsections as shown above. Each section is binarized separately based on local statistics. The regions 1-4 are easier to binarize. The regions 5-8 needs more processing to determine the threshold needed to binarize them. The threshold is chosen as the grey level at the location of the maximum slope as shown in Fig. 4. After each segment is binarized,

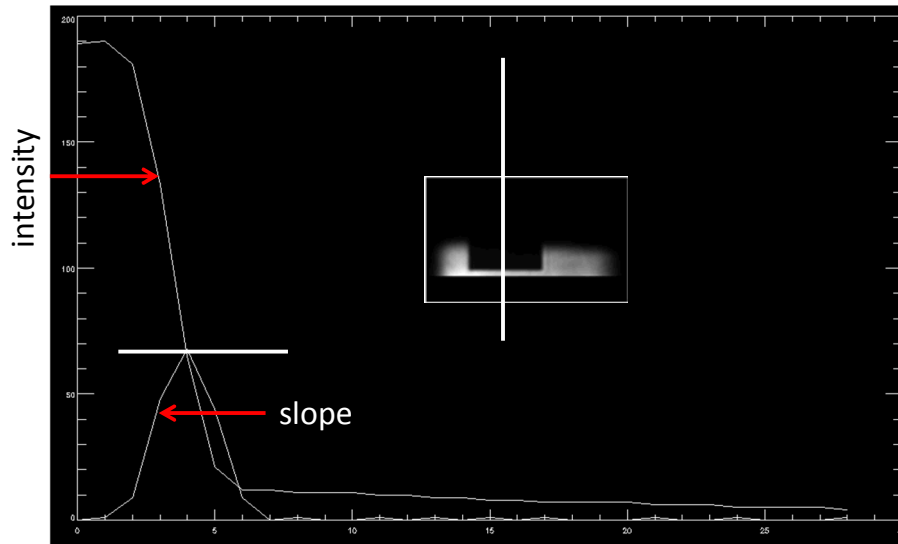


Figure 4: Intensity distribution along a vertical line and location of the maximum slope

they are combined together as shown in Fig. 5. Next, the sizes of the different isolated regions are classified based on their pixel count. If the radii of the circles vary between range  $r_1$  and  $r_2$ , their sizes will vary between  $\pi r_1^2$  and  $\pi r_2^2$ . By design the circles are usually smaller than the squares.

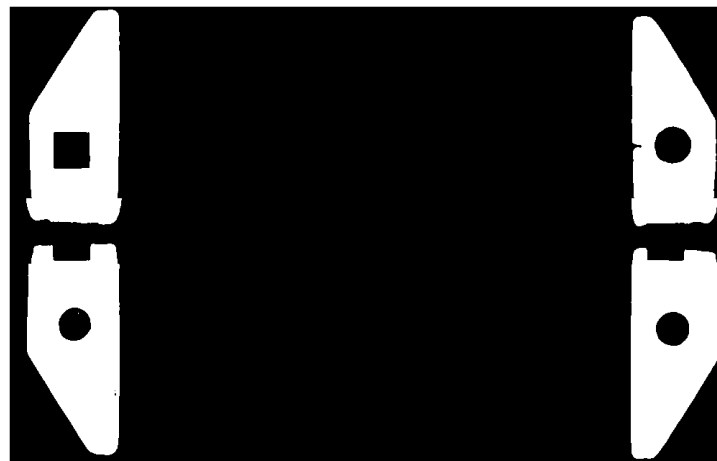


Fig. 5: The binarized ARC PAM SBI image.

As shown in the algorithm output below, the blob sizes are 1722, 1617, 2056 and 2541. The first three are expected to be those of the circles and blob size 2541 belongs to the square. Next, the best match template for the circles, from the small region containing the circle, is determined. This is done by searching over a range of radius and choosing the radius corresponding to the best match. Note that at this stage only one of the three circles is matched.

```

Blob classification based on size on binary images..
Looking for features in the range      600.625 to      3363.50
Feature sizes of interest      1722      1617      2542      2056
Found      4 spots in the valid range
For blob 1722, x = 915.00 y = 196.00 sq_side = 41.50 or rad = 23.41
For blob 1617, x = 81.00 y = 202.50 sq_side = 40.21 or rad = 22.69

```

```

For blob 2542, x = 77.50 y = 444.00 sq_side = 50.42 or rad = 28.45
For blob 2056, x = 913.50 y = 451.50 sq_side = 45.34 or rad = 25.58
Searching for square around 77.5000 444.000
Searching for big circles at 81.0000 202.500
Chosen Circle radius = 22.5000 Chosen Square side = 24.5000

```

After selecting the template for each type of fiducial, the whole image is correlated with the template to find the location of that particular fiducial. In addition, the detection accuracy is increased by using the edges of the each fiducial. It may

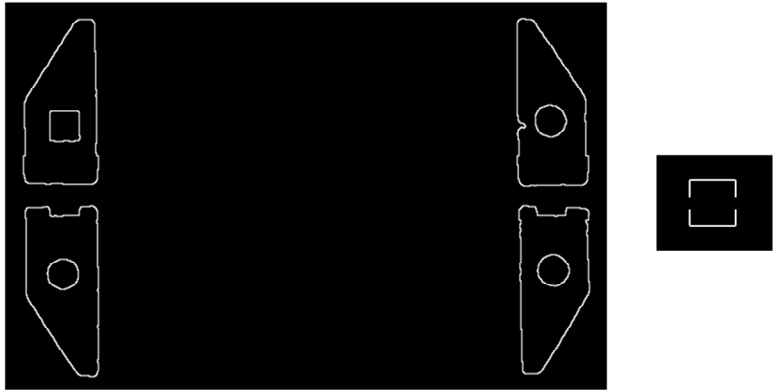


Fig. 6: The edge image generated from image of figure 5

be noted that the square fiducial is not completely square for the center most squares. The vertical edges of the square template is broken to match the center squares. Even then the squares produce a less than 50% correlation peak for some of these partially obstructed squares fiducial as shown below. The top left correlation is strongest as shown in the left figure of Fig. 7.

```

Looking for the outer squares with dimension 24.5000
xpos = 77.56, ypos = 444.14 Quality = 1.00 spots = 1
Top left square found, now creating mask...
xpos = 903.87, ypos = 316.99 Quality = 0.57 spots = 2
xpos = 77.94, ypos = 315.60 Quality = 0.47 spots = 3
*****Minimum quality factor accepted = 0.300000 and present 0.468889

```

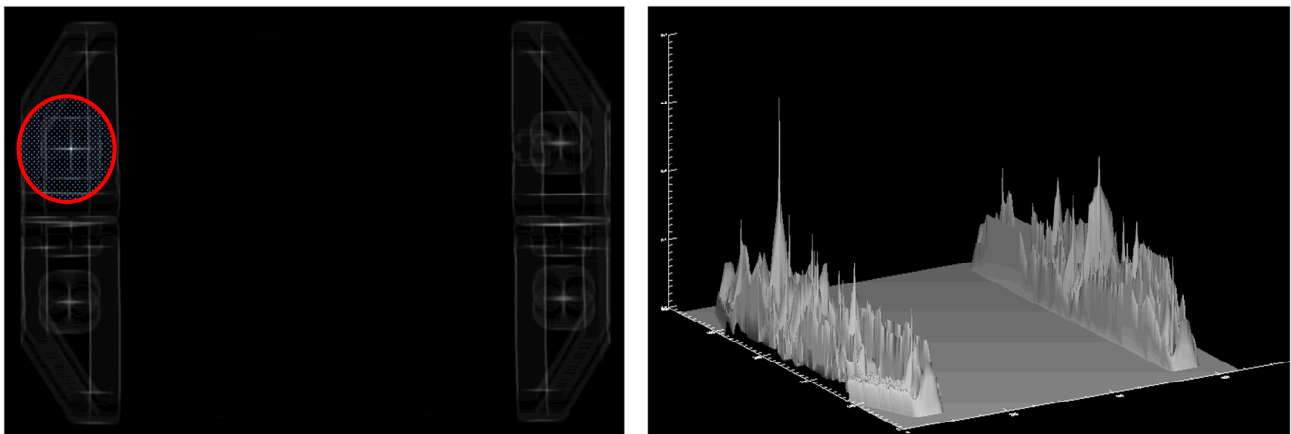


Figure 7. Detecting the squares, the correlation of the square with the image in Fig. 6

Note that to isolate the square peaks an additional mask is used in the square selection process. A mask is created as shown in the left image of Fig. 8, using apriori knowledge about the possible location of the squares. After multiplying the correlation plane and removing the first peak the next two peaks are clearly shown in Fig. 8 and their values are as shown in the text above Figure 7.

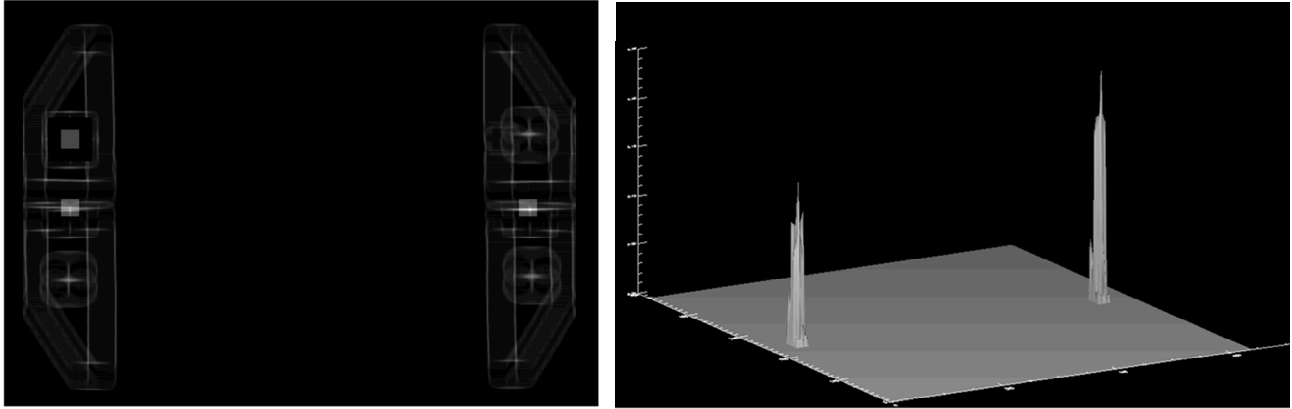


Figure 8. Detecting the square fiducial using a mask

Now using the edge of the first circles as filters, positions of all the three circles are obtained. This post processing step is used to validate any detected pattern as circles. The validation tests are 1) the spacing test on individual positions; 2) absolute position test for each of these positions and 3) spacing and position test taking a pair of locations at a time. The spacing test dictates that each circle must have two other circles at a certain x and y position interval. An absolute position test validates that the top left circle should be within the top one third of the area of the image. The pair test ensures that two squares should have the same y and a certain x distance. The output of the algorithm from these tests is shown below:

```

Looking for the circular spots with x_spacing      830.800 and y_spacing
      254.200 with tolerance 10-12%      83.0800      30.5040
Found      3 circle spots after spacing test
Looking for the square spots with x_spacing      830.800 and y_spacing
      127.100 with tolerance 10-12%      83.0800      15.2520
Found      3 square spots after spacing test
Passing manual position check .....
Passing redundant check for circles (2 at a time)...
Passing redundant check for squares (2 at a time)...
-----
Found      6 viable spots after triple tests ...

arc_ref_squares_beam_circles_eh:
  111.875      581.301      1.99000
  943.837      830.133      1.99000
  107.937      694.596      1.99000
  933.866      695.987      1.99000
  107.563      823.145      1.99000
  943.908      574.942      1.99000

```

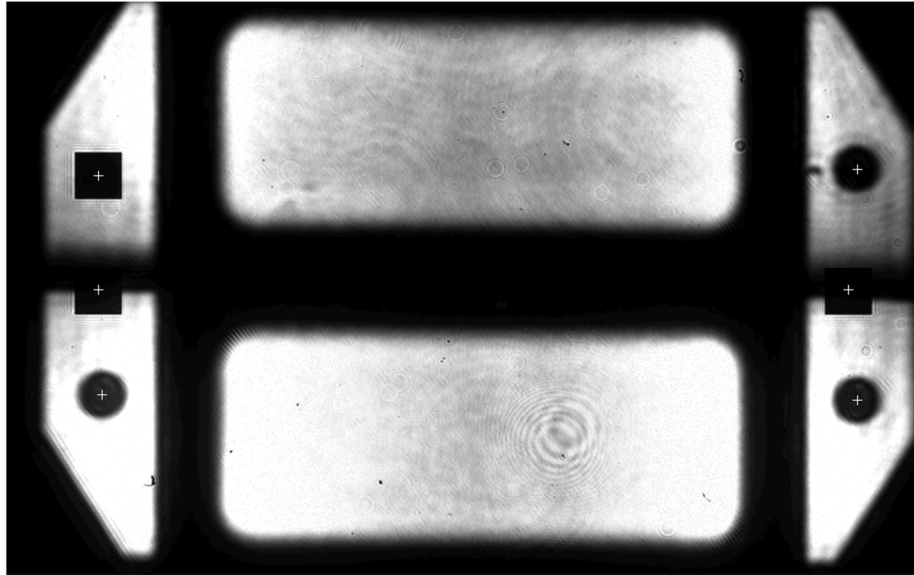


Figure 9. The ARC SBI PAM image with fiducial location

The locations of the 6 spots and their corresponding uncertainty are shown above. All the steps of the algorithm are shown in the block diagram of Figure 10. The steps of circle refinement is explained in the next section.

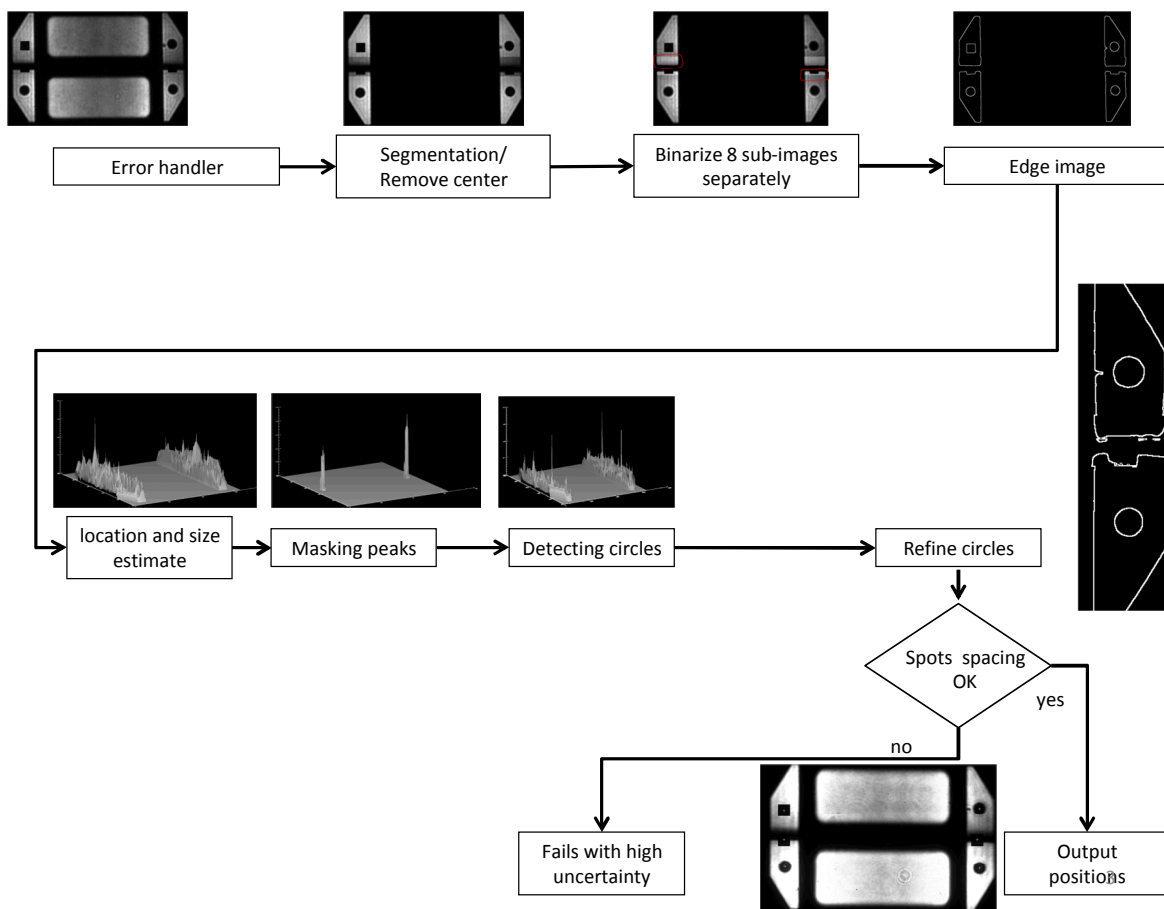


Figure 10: The ARC PAM split beam image processing algorithm

### 3. CIRCLE POSITION REFINEMENT

When we determine the size of the circle template, we only use one of the three circles. Due to the specific imaging condition, the size of the other circles may vary. As a result, when correlating the whole image with the template it may have weak correlation with the other circles. It may also lead to incorrect position determination. In order to increase the robustness, a second refinement is performed as explained below. The correlation output, due to the circle template, is shown in Figure 11. However, a close up of the peaks shown in Fig. 12 indicate that there is a size mismatch of the left and right circles, resulting in a correlation peak which itself is another circle. For a perfect match, the peak should be very bright with solid bright spot. In the refinement step, the size of the circle template for each of the spot locations is recalculated by selecting a small region around that initial circle location. Each individual location is then calculated from the subimage and their absolute location is calculated from the displacement of the subimage with respect to the origin of the whole image.

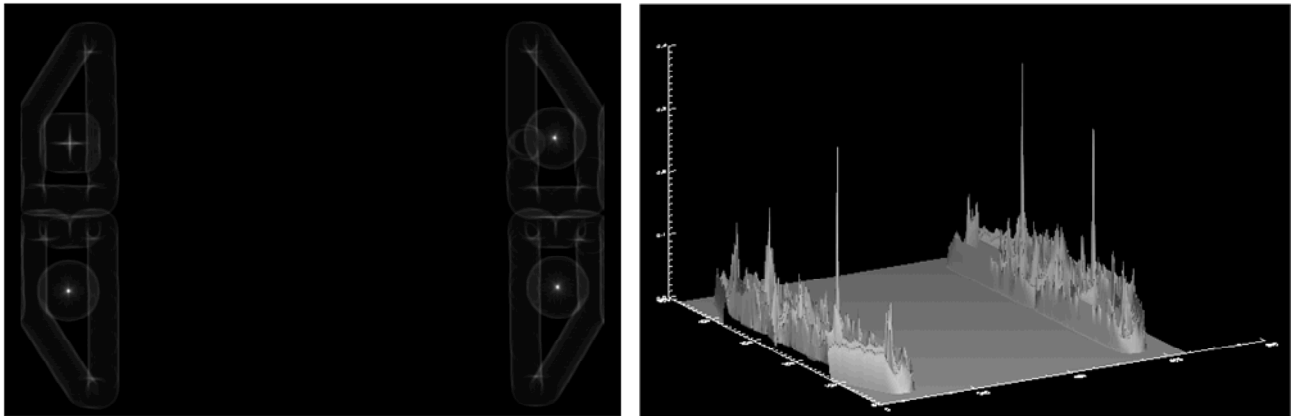


Figure 11. The correlation output from the circle template

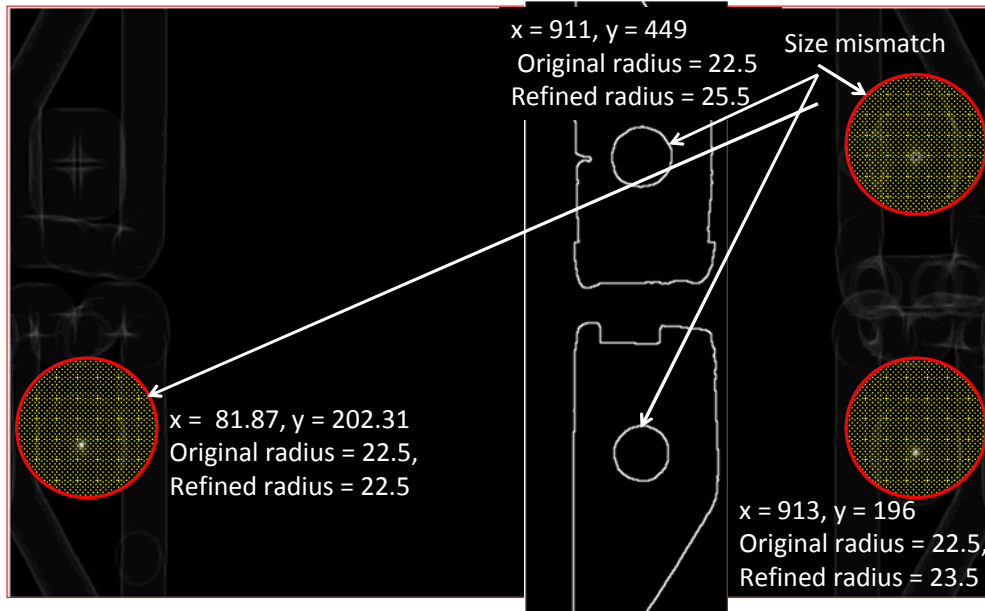


Figure 12. Close-up of the circle correlation output shows broad correlation for two right circles

The algorithm output below shows the circles on the right wing show a refined radius of 23.5 and 25.5 pixels.

```

Looking for the outer circles with radius      22.5000
xpos = 81.88, ypos = 202.30 Quality = 1.00 spots = 4
Original radius = 22.5, Refined radius = 22.5
xpos = 913.81, ypos = 195.92 Quality = 0.81 spots = 5
Original radius = 22.5, Refined radius = 23.5
xpos = 910.86, ypos = 448.78 Quality = 0.42 spots = 6
Original radius = 22.5, Refined radius = 25.5
*****Minimum quality factor accepted = 0.50 and present
0.422914
Possible      3 squares and      3 circles found.....

```

#### 4. CONCLUSIONS

In this paper, a method of detecting fiducials for ARC SBI PAM images is described. One main challenge of this is the missing part of the square fiducials. A subimaging technique is used to binarize the SBI image using local statistics. Instead of using a complete square, a partial square is used as the template for the partially missing squares. A refinement method is used for the circle fiducials when there is a left to right variation in the size of the circles.

#### ACKNOWLEDGEMENT

This work performed under the auspices of the U.S. Department of Energy by Lawrence Livermore National Laboratory under Contract DE-AC52-07NA27344. AASA acknowledges useful comments by Gordon Brunton.

#### REFERENCES

- [1] Special issue of Physics of Plasmas on "Plans for the National Ignition campaign (NIC) on the National Ignition Facility (NIF): On the threshold of initiating ignition experiments," guest edited by John Lindl and Edward I. Moses, 5, (2011); see also p. 050901-1 for an overview editorial.
- [2] R. S. Roberts, et al., "Image analysis for the automated alignment of the advanced radiography capability (ARC) diagnostic path," Proceedings of the International Conference on Accelerator and Large Experimental Physics Control Systems (ICALEPCS), 1274-1277 (2013).
- [3] S. C. Burkhart, E. Bliss, D. Kalantar, R. Lowe-Webb, T. McCarville, D. Nelson, ... K. Wilhelmsen, "National Ignition Facility system alignment," *Applied Optics*, 50(8), 1136-57 (2011).
- [4] K. Wilhelmsen, A. Awwal, W. Ferguson, B Horowitz, V. Miller Kamm, C. Reynolds, "Automatic Alignment System For The National Ignition Facility", Proceedings of 2007 International Conference on Accelerator and Large Experimental Control Systems (ICALEPCS07), 486-490, Knoxville, Tennessee (2007).
- [5] J. V. Candy, W. A. McClay, A. A. S. Awwal, and S. W. Ferguson, "Optimal position estimation for the automatic alignment of a high-energy laser," *Journal of Optical Society of America A*, Vol. 22, pp. 1348-1356 (2005).
- [6] M. A. Karim and A. A. S. Awwal, *Optical Computing: An Introduction*, John Wiley, New York, NY, 1992.
- [7] A. A. S. Awwal, "What can we learn from the shape of a correlation peak for position estimation?," *Applied Optics*, Vol. 49, pp. B41-B50, April 1, (2010).
- [8] J.V. Candy, A. A. S. Awwal, W. McClay, S. C. Burkhart, "Detection of off-normal images for NIF automatic alignment," in *Photonic Devices and Algorithms for Computing VII*, edited by K. Iftekharuddin and A. A. S. Awwal,, Proc. of SPIE Vol. 5907, 59070B-1 - 59070B-12, (2005).
- [9] A. A. S. Awwal, Wilbert A. McClay, Walter S. Ferguson, James V. Candy, Thad Salmon, and Paul Wegner, "Detection and Tracking of the Back-Reflection of KDP Images in the presence or absence of a Phase mask," *Applied Optics*, Vol. 45, pp. 3038-3048, (2006).
- [10] W. A. McClay III, et al., "Evaluation of laser-based alignment algorithms under additive random and diffraction noise," in *Photonic Devices and Algorithms for Computing VI*, edited by K. Iftekharuddin and A. A. S. Awwal, Proc. of SPIE 5556 (SPIE Bellingham, WA, 2004), pp. 243-248.